

of the previously known N<sup>15</sup> levels show up as distinct slow-neutron thresholds. This result is not too surprising for one would expect sharp thresholds only for those N<sup>15</sup> states for which the compound nucleus level had a large reduced width for *s* wave neutron emission. More puzzling is the fact that the two strongest and sharpest observed thresholds,  $E_d=2.036$  and  $2.227$  Mev, do not correspond to any previously observed N<sup>15</sup> level. However, the only previous data on N<sup>15</sup> levels in this region come from M. I. T. magnetic spectrometer data<sup>14</sup> on N<sup>14</sup>(d,p)N<sup>15</sup>. Unfortunately their nitrogen target (nylon) contained enough carbon that the prominent proton groups from C<sup>12</sup>(d,p) reactions to the 3.855- and 3.684-Mev states of C<sup>13</sup> completely swamp the plate region

<sup>14</sup> A. Sperduto, W. W. Buechner, C. K. Bockelman, and C. P. Browne, *Phys. Rev.* **96**, 1316 (1954).

where these N<sup>15</sup> groups would be expected to occur. (See, e.g., their Figs. 1 and 4.)

Since the threshold at  $E_d=2.393$  Mev occurs at the same energy as the O<sup>16</sup>(d,n) threshold to the first excited state of F<sup>17</sup> (see Fig. 11), oxygen contamination of the target must be considered. Absence of the much stronger O<sup>16</sup>(d,n)F<sup>17</sup> ground-state threshold ( $E_d=1.832$  Mev) excludes this possibility.

#### ACKNOWLEDGMENTS

The author wishes to express thanks to Professor Hugh T. Richards who suggested and guided this work. The author would also like to thank Dr. William R. Phillips and Dr. E. A. Silverstein for their assistance in taking data.

## Neutrons and Gamma Rays from the Bombardment of O<sup>16</sup> by He<sup>3</sup>

K. L. DUNNING AND J. W. BUTLER

*Nucleonics Division, U. S. Naval Research Laboratory, Washington, D. C.*

(Received April 11, 1961)

The threshold energy for the O<sup>16</sup>(He<sup>3</sup>,n)Ne<sup>18</sup> reaction has been measured. The value obtained,  $3.811\pm0.015$  Mev, determines the mass of Ne<sup>18</sup> to be  $18.011446\pm0.000014$  amu (O<sup>16</sup> standard, 1960 mass tables). The slow-fast ratio method for the observation of neutron thresholds was employed at bombarding energies from the ground-state threshold to 5.6 Mev, corresponding to a region of excitation in the residual nucleus from zero to 1.5 Mev. No excited states in Ne<sup>18</sup> were identified. The bombardment of O<sup>16</sup> by He<sup>3</sup> also produced the reactions O<sup>16</sup>(He<sup>3</sup>,p)F<sup>18</sup> and O<sup>16</sup>(He<sup>3</sup>,α)O<sup>15</sup>.

Energy spectra were obtained by means of a scintillation spectrometer for gamma rays resulting from certain transitions in F<sup>18</sup> and O<sup>15</sup>. For 4.5-Mev He<sup>3</sup> particles impinging on a 1-Mev thick target of TiO<sub>2</sub>, gamma rays of the following energies were observed and attributed to F<sup>18</sup>:  $0.652\pm0.007$ ,  $0.939\pm0.005$ ,  $1.041\pm0.005$ ,  $1.17\pm0.01$ ,  $1.61\pm0.02$ ,  $1.68\pm0.02$ ,  $2.09\pm0.01$ ,  $2.51\pm0.01$ ,  $2.65\pm0.05$ ,  $3.06\pm0.05$ ,  $3.35\pm0.10$ ?, and  $3.84\pm0.10$  Mev. The following gamma rays were also observed and attributed to O<sup>15</sup>:  $5.25\pm0.05$ ,  $6.22\pm0.10$ , and  $6.87\pm0.10$  Mev.

#### INTRODUCTION

THE first experimental evidence for Ne<sup>18</sup> was reported by Gow and Alvarez<sup>1</sup> who produced it in the reaction F<sup>19</sup>(p,2n)Ne<sup>18</sup>, and found it to be a positron emitter with an end point of  $3.2\pm0.2$  Mev, a half-life of  $1.6\pm0.2$  sec, and a  $\log ft$  value of  $2.9\pm0.2$ . In the present experiment, the reaction O<sup>16</sup>(He<sup>3</sup>,n)Ne<sup>18</sup> has been used to determine the mass of Ne<sup>18</sup> by means of a ground-state threshold measurement and also to search for excited states of Ne<sup>18</sup>. Bombarding energies up to 5.6 Mev have been used. Also, energy spectra have been obtained for gamma rays arising from the reactions O<sup>16</sup>(He<sup>3</sup>,p)F<sup>18</sup> and O<sup>16</sup>(He<sup>3</sup>,α)O<sup>15</sup> at a bombarding energy of 4.5 Mev. These gamma rays have been correlated to transitions in F<sup>18</sup> and O<sup>15</sup>. A preliminary report has been made on part of this work.<sup>2</sup>

#### EXPERIMENTAL PROCEDURE

Four thin targets and one fairly thick target of O<sup>16</sup> were bombarded with the magnetically analyzed singly-

charged He<sup>3</sup> beam from the NRL 5-Mv Van de Graaff accelerator. The energy spread in the beam was about  $\frac{1}{3}\%$ . The neutron yields from the four thin targets were examined with the counter-ratio method, as a function of the bombarding energy. The apparatus and procedures used for these measurements have been described previously.<sup>3,4</sup> The gamma rays resulting from the bombardment of the fairly thick target with a 4.50-Mev beam were detected in a 3-in.×3-in. NaI(Tl) crystal mounted on a type-6363 multiplier phototube after they had passed through a composite shield designed to reduce the intensity of x rays and annihilation radiation relative to that of higher-energy radiation. The materials through which the gamma rays passed after leaving the target and before entering the NaI crystal were as follows, and are given in the order of flight: stainless steel, 0.025 in. (target chamber wall); paraffin, 0.25 in.; lead, 0.31 in.; tantalum, 0.016 in.; cadmium, 0.012 in.; zinc, 0.010 in.; aluminum, 0.031 in.

<sup>3</sup> K. L. Dunning, R. O. Bondelid, and J. W. Butler, *Phys. Rev.* **110**, 1076 (1958).

<sup>4</sup> J. W. Butler, K. L. Dunning, and R. O. Bondelid, *Phys. Rev.* **106**, 1224 (1957).

<sup>1</sup> J. D. Gow and L. W. Alvarez, *Phys. Rev.* **94**, 365 (1954).

<sup>2</sup> K. L. Dunning and J. W. Butler, *Bull. Am. Phys. Soc.* **4**, 444 (1959).

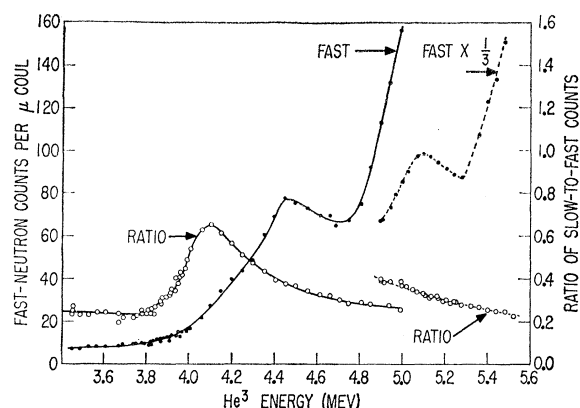


FIG. 1. Excitation curve for the reaction  $O^{16}(He^3, n)Ne^{18}$ , showing the yield of fast neutrons (closed circles) and the ratio of slow-to-fast counts (open circles). The solid lines are for a CaO target about 70 kev thick to 4.5-Mev  $He^3$  particles, and the broken lines are for a slightly thicker CaO target. No background has been subtracted.

(crystal case); magnesium oxide, 0.23 in. (reflector). The target and gamma-ray detector were surrounded with a lead shield 4 in. thick, except at the  $He^3$  drift tube entry point, for background radiation reduction. The gamma-ray pulses were sorted with a 100-channel pulse-height analyzer which was calibrated with radioactive sources  $Na^{22}$ ,  $Co^{60}$ , and the 4.43-Mev gamma ray from a Po-Be neutron source.

The first target bombarded was 70 kev thick to 4.5-Mev  $He^3$  particles. It was made by electrodeposition of calcium from a solution of  $Ca(NO_3)_2$  in ethyl alcohol onto a platinum blank 0.010 in. thick. The blank and its deposit were then heated in an oven, in an atmosphere of oxygen, to a maximum temperature of 2400°F. The heating time was about 2 hr, including the time required for the oven to warm up and cool down. The second target, about 110 kev thick to 4.5-Mev  $He^3$  particles, was made in a similar way except that, after electrodeposition, the blank and deposit were brought to a white heat for a few minutes in air with an oxygen-

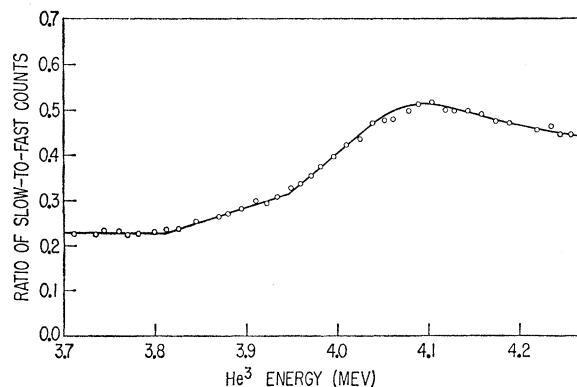


FIG. 2. Ratio of slow-to-fast counts for the energy region 3.70-4.27 Mev. The target was of CaO and about 15 kev thick to 4.5-Mev  $He^3$  particles. No background has been subtracted.

natural-gas flame. The third target was made in a manner similar to the first, and was 10 to 15 kev thick to 4.5-Mev  $He^3$  particles. The fourth target was formed by the deposition of a suspension of  $TiO_2$  in water onto a platinum blank and was about 30 kev thick. The water was then evaporated slowly by means of a heat lamp. The blank and deposit were then purged of contaminants in an oxygen atmosphere in the oven as described for the first target.

The fifth target, which was about 1 Mev thick to 4.5-Mev  $He^3$  particles, was formed through the deposition of a suspension of 2 mg  $cm^{-2}$  of  $TiO_2$  in an alcohol binder onto a platinum blank 0.010 in. thick, which had been heated in an atmosphere of air for 1 hr at 2500°F. The blank and the deposit were then heated in an atmosphere of oxygen at 2600°F for about 2.5 hr.

## RESULTS

Figure 1 is a plot of the fast neutron counts and of the slow-to-fast ratio for a variation of the energy of the incident  $He^3$  particles through the range 3.4-5.6 Mev. The solid curves indicate data taken with the 70-kev

TABLE I. Information related to the ground-state threshold bombarding energy for the reaction  $O^{16}(He^3, n)Ne^{18}$ , based on the mass tables of reference 5 ( $O^{16}$  standard).

Ground-state threshold bombarding energy	3.811	$\pm 0.015$	Mev
Ground-state $Q$ value	-3.206	$\pm 0.013$	Mev
Mass of $Ne^{18}$	18.011446	$\pm 0.000014$	amu
Mass excess of $Ne^{18}$	10.658	$\pm 0.013$	Mev
End-point energy of positron spectrum $Ne^{18}$ (for decay to the ground state of $F^{18}$ )	3.423	$\pm 0.02$	Mev

target; the broken curves indicate data taken with the 110-kev target. The statistical uncertainties for the points on the ratio curve of Fig. 1 are about twice the size of the open circles below threshold and somewhat smaller for the remainder of the curve.

The rise in the ratio curve beginning about 3.8 Mev is interpreted as being due to the formation of the ground state of  $Ne^{18}$ . A careful examination of the ratio curve shows that the rise appears to break upward at about 3.95 Mev. Figure 2 shows the results of a more careful investigation of the region from 3.70 to 4.26 Mev; these data were obtained with the target which was 10 to 15 kev thick. The statistical uncertainties near the break in the rising part of the curve are about half the size of the open circles. This break, though appearing to be quite definite, is interpreted as being due to an excited state or group of excited states in the compound nucleus,  $Ne^{19}$ , rather than an excited state in the residual nucleus,  $Ne^{18}$ .

As a check on the possibility that the neutron threshold at 3.811 Mev and the break at 3.95 Mev were due to some contaminant on the target (or perhaps the Ca) and not due to  $O^{16}$ , the 30-kev target of  $TiO_2$  was bom-

barded. This target gave essentially the same results as those shown in Fig. 2.

The probability that the interesting features of the ratio curve were caused by the presence of a contaminant in the beam (such as  $HD^+$  ions) is very small since a number of precautions were taken to avoid beam contamination. The  $He^3$  was purified with activated charcoal prior to use. The ion source and accelerating tube never had been used to accelerate any particle other than  $He^3$  prior to the present experiment.

The smoothness of the fast-neutron curve and an examination of a plot of the slow-neutron yield, which is not shown, indicate that the rises in the ratio curve at threshold and at the break at 3.95 Mev are due to the production of slow neutrons.

The data of Fig. 2 indicate that the neutron threshold for  $Ne^{18}$  is at  $3.811 \pm 0.015$  Mev. This threshold energy determines the mass excess of  $Ne^{18}$  to be  $10.658 \pm 0.013$  Mev relative to the values given for  $He^3$  and the neutron by Everling *et al.*<sup>5</sup> in their 1960 mass tables ( $O^{16}$

TABLE II. Gamma rays resulting from the bombardment of  $O^{16}$  by  $He^3$ , listed according to the reaction from which each gamma ray originated.

$O^{16}(He^3, p)F^{18}$ (Mev)	$O^{16}(He^3, \alpha)O^{15}$ (Mev)
$0.652 \pm 0.007$	$5.25 \pm 0.05$
$0.939 \pm 0.005$	$6.22 \pm 0.10$
$1.041 \pm 0.005$	$6.87 \pm 0.10$
$1.17 \pm 0.01$	
$1.61 \pm 0.02$	
$1.68 \pm 0.02$	
$2.09 \pm 0.01$	
$2.51 \pm 0.01$	
$2.65 \pm 0.05$	
$3.06 \pm 0.05$	
$3.35 \pm 0.10^?$	
$3.84 \pm 0.10$	

standard). This value may be compared with the value of the mass excess of  $Ne^{18}$  given in these mass tables,  $10.430 \pm 0.200$  Mev. Other information related to this threshold energy is given in Table I.

The peaks in the fast neutron curve of Fig. 1 imply that there is resonant compound nucleus formation when  $O^{16}$  is bombarded with  $He^3$  particles in this energy range, but since only one angle was observed, this explanation for the peaks is not unique. Bromley *et al.*<sup>6</sup> found strong evidence for resonances in their studies of the mechanism of the reaction  $O^{16}(He^3, \alpha)O^{15}$  at somewhat lower bombarding energies.

Figures 3 and 4 show gamma-ray spectra obtained at a bombarding energy of 4.5 Mev with the target which was 1 Mev thick. Table II gives the energies of the observed gamma rays and the reaction to which they are attributed. Figure 5 is a level diagram of  $F^{18}$

<sup>5</sup> F. Everling, L. A. König, J. H. E. Mattauch, and A. H. Wapstra, *Nuclear Phys.* **18**, 529 (1960).

<sup>6</sup> D. A. Bromley, J. A. Kuehner, and E. Almqvist, *Nuclear Phys.* **13**, 1 (1959).

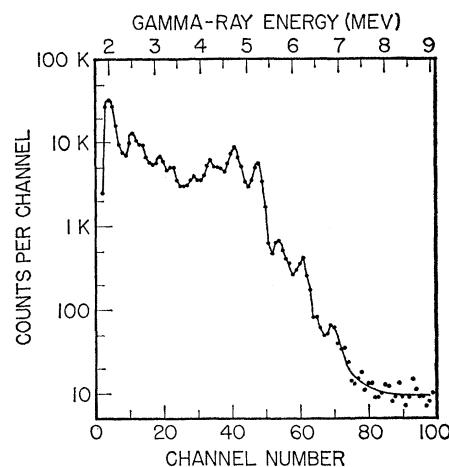


FIG. 3. Energy spectrum of the prompt gamma rays from  $O^{16}+He^3$  at a bombarding energy of 4.5 Mev with the gain adjusted so that channel 100 corresponds to a gamma-ray energy just above 9 Mev. No background has been subtracted.

showing the transitions which are believed to have given rise to those observed gamma rays attributed to  $F^{18}$ . The level energies, spins, and parities are those listed by Ajzenberg-Selove and Lauritsen<sup>7</sup> with the following exceptions. The isobaric spin and parity assignments of the 1.085-Mev level have been interchanged with those of the 1.043-Mev level because of the results of a recent study<sup>8</sup> of the way in which  $Ne^{18}$  decays to low-lying states in  $F^{18}$ . The gamma-ray energies as measured in the present experiment are shown along the vertical arrows. The energy of the 3.35-Mev transition is enclosed in parentheses, and the arrow to it (indicating excited-state population) is broken to signify that this assignment is uncertain.

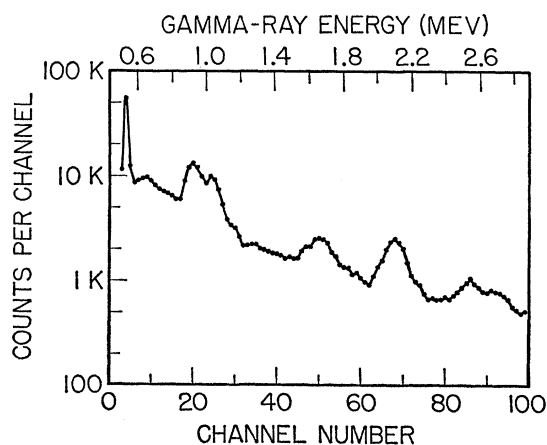


FIG. 4. Energy spectrum of the prompt gamma rays from  $O^{16}+He^3$  at a bombarding energy of 4.5 Mev with the gain adjusted so that channel 100 corresponds to a gamma-ray energy just above 2.8 Mev. No background has been subtracted.

<sup>7</sup> F. Ajzenberg-Selove and T. Lauritsen, *Nuclear Phys.* **11**, 1 (1959).

<sup>8</sup> J. W. Butler and K. L. Dunning, *Phys. Rev.* **121**, 1782 (1961).

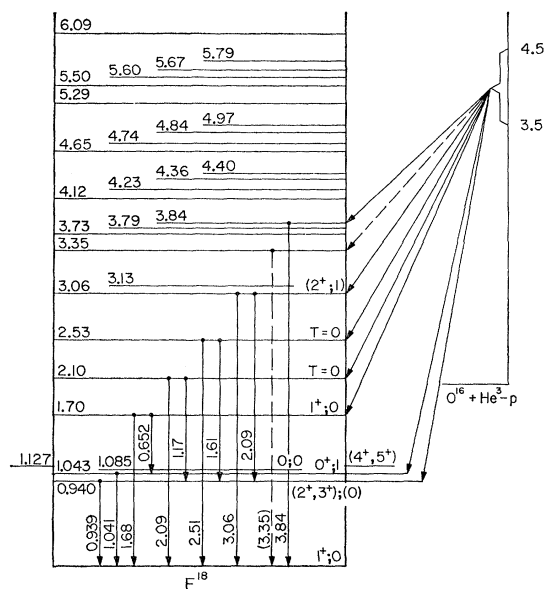


FIG. 5. Energy level diagram of  $F^{18}$ . The level energies are those of reference 7. The transition energies are those measured in the present experiment. The range of bombarding energies in the target are shown on the right-hand side in the scale of the center-of-mass system, but labeled with values in the laboratory system.

Many gamma-ray spectra were taken, but the interesting features of all of them are illustrated by those of Figs. 3 and 4; an interpretation of these features follows. The highest energy peak of Fig. 3 ( $6.87 \pm 0.10$  Mev) is mainly the photopeak of the ground-state transition from the 6.86-Mev state in  $O^{15}$  (see reference 7 for an energy-level diagram of  $O^{15}$  and a list of references to the original literature). The inflection point at about 6.35 Mev is due to the "single-escape" peak of the 6.87-Mev gamma ray. The peak at  $6.22 \pm 0.10$  Mev is mainly the photopeak of a ground-state transition from the 6.15-Mev state in  $O^{15}$ . The 5.70-Mev peak is a combination of the "double-escape" peak from the 6.86-Mev transition and the single-escape peak from the 6.15-Mev transition. The two lowest-lying states reported<sup>9</sup> in  $O^{15}$  are at 5.20 and 5.25 Mev. The peak of Fig. 3 at  $5.25 \pm 0.05$  Mev is very likely a combination of the photopeaks due to the ground-state transitions from these states and contains a contribution from the double-escape peak from the 6.15-Mev transition. The peaks at 4.74 and 4.23 Mev are, respectively, the single-escape and double-escape peaks associated with the transitions of about 5.25 Mev.

The peaks of Fig. 3 which are of lower energy than those mentioned are attributed to transitions in  $F^{18}$ , except the one at 2 Mev (channel 5), which is of electronic origin. The peak at  $3.84 \pm 0.10$  Mev is the photopeak of a ground-state transition from the 3.84-Mev state in  $F^{18}$ . It is not clear from the present data whether the peak at  $3.35 \pm 0.10$  Mev is a combination of the

photopeak of a 3.35-Mev gamma ray and the single-escape peak of the 3.84-Mev gamma ray, or is entirely due to the latter. If there is a contribution from a 3.35-Mev gamma ray, it probably arises from a ground-state transition from the 3.35-Mev state. The peak at  $3.06 \pm 0.05$  Mev is interpreted as the photopeak associated with a ground-state transition from the 3.06-Mev state. The double-escape peak of the 3.84-Mev transition and the single-escape peak of the 3.35-Mev transition should lie at about 2.83 Mev; they are apparently concealed in the skirts of the peak at  $2.65 \pm 0.05$  Mev which also appears in Fig. 4. The origin of this last-mentioned peak is very uncertain, since it contains, in addition to the aforementioned sources, contributions from either or both of the following: 3.79-Mev state to the 1.127-Mev state (2.66-Mev transition) and 3.73-Mev state to the 1.085-Mev state (2.65-Mev transition). The peak at  $2.51 \pm 0.01$  Mev is assigned to the ground-state transition from the 2.53-Mev state. The peak in Fig. 4 at  $2.09 \pm 0.01$  Mev is composed of the ground-state transition from the 2.10-Mev state and the photopeak of a transition from the 3.06-Mev state to the 0.940-Mev state with contributions from the double-escape peak from the 3.06-Mev ground-state transition and the single-escape peak from the 2.52-Mev transition. The peak at  $1.68 \pm 0.02$  Mev is the ground-state transition from the 1.70-Mev state. The peak at  $1.61 \pm 0.02$  Mev is probably due mainly to the transition from the 2.53-Mev state to the 0.940-Mev state, with contributions from the double-escape peak from the 2.53-Mev ground-state transition and the single-escape peak from the 3.06-to-0.94 Mev transition. The peak at  $1.17 \pm 0.01$  Mev is mainly the photopeak of a transition from the 2.10-Mev state to the 0.940-Mev state, with a small contribution from the single-escape peak from the 1.70-Mev ground-state transition and from the double-escape peak of the 3.06-to-0.94 Mev transition. The peaks at  $1.041 \pm 0.005$  Mev and  $0.939 \pm 0.005$  Mev are the photopeaks of the ground-state transitions from the 1.043-Mev and 0.940-Mev states, respectively. The peak at  $0.652 \pm 0.007$  Mev is the photopeak of a transition from the 1.70-Mev state to the 1.043-Mev state. Finally, the peak at 0.51 Mev is due to annihilation radiation.

## DISCUSSION

The  $Q$  value of  $-3.206 \pm 0.013$  Mev is in good agreement with the value  $-3.199 \pm 0.006$  Mev obtained by Towle and Macefield,<sup>10</sup> who investigated the  $O^{16}(He^3, n)Ne^{18}$  reaction by means of neutron-threshold and time-of-flight techniques with bombarding energies up to 10 Mev. Ajzenberg-Selove and Dunning<sup>11</sup> measured the  $Q$  value to be  $-3.20 \pm 0.05$  Mev in their investigation of this reaction using 5.52-Mev  $He^3$  particles and nuclear emulsion detectors.

<sup>10</sup> J. H. Towle and B. E. Macefield (private communication).

<sup>9</sup> B. Povh, Phys. Rev. **114**, 1114 (1959); D. F. Hebbard and B. Povh, Nuclear Phys. **13**, 642 (1960).

<sup>11</sup> F. Ajzenberg-Selove and K. L. Dunning, Phys. Rev. **119**, 1681 (1960).

The rate of rise of the ratio curve after threshold for the present experiment (see Fig. 2) is much less than for other reactions<sup>3,4</sup> investigated with the same apparatus and geometry. For example, the  $Li^6(He^3,n)B^8$  ratio curve<sup>3</sup> rose to a maximum within 15 kev after threshold (for a target about 14 kev thick at threshold). The ratio curve of the present experiment rises very slowly by comparison, finally reaching a maximum about 300 kev above threshold. The shape of the ratio curve above threshold is determined by the cross section for the reaction, the target thickness, the variation of the efficiencies of the neutron counters with neutron energy, the rate at which the neutron cone opens as a function of energy, and the relative effective solid angle subtended at the target by the detectors. The most reasonable cause for the long slow rise appears to be the reaction cross section as a function of bombarding energy.

The upward break in the ratio curve at 3.95 Mev could conceivably be interpreted as the threshold for a new excited state in  $Ne^{18}$ . In the preliminary report<sup>2</sup> on a part of the present experiments, this break in the ratio curve was noted, and it was stated that if this break did correspond to a neutron threshold, the energy of the residual excited state would be 114 kev. The existence of this break so near the ground-state threshold is in itself very weak evidence for a low-lying excited state in the residual nucleus because, in previous experiments,<sup>3,4</sup> "satellites" of true neutron thresholds have been observed about 100 kev above the true threshold. Since there is no independent evidence for such a low-lying state in  $Ne^{18}$ , it appears more reasonable to attribute this break to the same mechanism as that of the previously observed "satellites", i.e., resonances in the compound nucleus.

Since the ratio curve of Fig. 1 shows no evidence for any higher thresholds up to the maximum bombarding energy of 5.6 Mev (corresponding to a possible excitation energy of about 1.5 Mev), there is no evidence in the present experiment for excited states in  $Ne^{18}$  below 1.5 Mev. This observation is consistent with the work of Towle and Macefield,<sup>10</sup> who found three excited

states above this range but none within it. Further, there was no evidence in the work of Ajzenberg-Selove and Dunning<sup>11</sup> for excited states in the range of excitation energies of the present experiment. These findings are consistent with the reported energy-level scheme of the mirror nucleus,  $O^{18}$ , whose lowest excited state has an energy of 1.982 Mev.<sup>7</sup>

The gamma-ray energies, as measured in the present experiment, are consistent with the measurements of others as far as such comparisons can be made. Butler *et al.*<sup>12</sup> observed gamma rays for the same reaction but at a bombarding energy of 2 Mev. Their values of 2.49, 2.10, 1.69, 1.06, and 0.94 Mev correspond to five of the gamma-ray energies listed in Table II. Naggjar *et al.*,<sup>13</sup> using the  $O^{18}(p,n\gamma)F^{18}$  reaction, observed gamma rays of  $0.94 \pm 0.02$  and  $1.04 \pm 0.02$  Mev; these gamma rays arise from the same states as the 0.939- and 1.041-Mev gamma rays of the present experiment. Kuehner *et al.*<sup>14</sup> obtained values of 0.940 and 1.045 Mev for two of the gamma rays from the  $O^{16}(He^3,p\gamma)F^{18}$  reaction. Hinds and Middleton<sup>15</sup> measured the energies of the proton groups from the  $O^{16}(He^3,p)F^{18}$  reaction and the alpha-particle groups from the  $F^{19}(He^3,\alpha)F^{18}$  reaction at a bombarding energy of 5.9 Mev. Not every level observed by Hinds and Middleton was observed in the present experiment because of the better resolution of their magnetic proton spectrometer as compared with the scintillation gamma-ray spectrometer of the present experiment, and also because of their higher bombarding energy (5.9 Mev compared with an average energy of 4 Mev in the target for the present experiment). However, as seen in Fig. 5, most of the excited states below 4 Mev were observed in the present experiment.

<sup>12</sup> J. W. Butler, H. D. Holmgren, and W. E. Kunz, *Bull. Am. Phys. Soc.* **1**, 29 (1956).

<sup>13</sup> V. Naggjar, M. Roelawski-Conjeaud, D. Szteinszneider, and J. Thirion, *J. phys. radium* **17**, 561 (1956); D. Szteinszneider, M. Roelawski-Conjeaud, and V. Naggjar, *Compt. rend.* **244**, 445 (1957).

<sup>14</sup> J. A. Kuehner, E. Almqvist, and D. A. Bromley, *Phys. Rev. Letters* **1**, 260 (1958).

<sup>15</sup> S. Hinds and R. Middleton, *Proc. Phys. Soc. (London)* **73**, 721 (1959).